The Journal of Immunology

In Vivo Blockade of Macrophage Migration Inhibitory Factor Ameliorates Acute Experimental Autoimmune Encephalomyelitis by Impairing the Homing of Encephalitogenic T Cells to the Central Nervous System

Claudia M. Denkinger, Michael Denkinger, Jens J. Kort, Christine Metz and Thomas G. Forsthuber

J Immunol 2003; 170:1274-1282; ;
doi: 10.4049/jimmunol.170.3.1274
http://www.jimmunol.org/content/170/3/1274

The Journal of Immunology is published twice each month by
The American Association of Immunologists, Inc.,
1451 Rockville Pike, Suite 650, Rockville, MD 20852

Print ISSN: 0022-1767 Online ISSN: 1550-6606.

In Vivo Blockade of Macrophage Migration Inhibitory Factor Ameliorates Acute Experimental Autoimmune Encephalomyelitis by Impairing the Homing of Encephalitogenic T Cells to the Central Nervous System

Claudia M. Denkinger,*‡ Michael Denkinger,* Jens J. Kort,*† Christine Metz,§ and Thomas G. Forsthuber[2]*

Macrophage migration inhibitory factor (MIF) is a cytokine that plays a critical role in the regulation of macrophage effector functions and T cell activation. However, its role in the pathogenesis of T cell-mediated autoimmune diseases, such as experimental autoimmune encephalomyelitis (EAE), has remained unresolved. In this study, we report that anti-MIF Ab treatment of SJL mice with acute EAE improved the disease severity and accelerated the recovery. Furthermore, the anti-MIF treatment impaired the homing of neuroantigen-reactive pathogenic T cells to the CNS in a VCAM-1-dependent fashion. Interestingly, MIF blockade also decreased the clonal size of the neuroantigen-specific Th1 cells and increased their activation threshold. Taken together, the results demonstrate an important role for MIF in the pathogenesis of EAE/multiple sclerosis and suggest that MIF blockade may be a promising new strategy for the treatment of multiple sclerosis. ***The Journal of Immunology,*** **2003, 170: 1274–1282.**

Multiple sclerosis (MS)[3] is a chronic inflammatory and demyelinating disease of the CNS believed to be mediated by an autoimmune T cell attack on Ags present in the myelin sheath of the CNS, such as myelin basic protein, proteolipid protein (PLP), or myelin oligodendrocyte glycoprotein (1–3). To induce the disease, primed, autoreactive T cells must migrate to the CNS and recognize neuroantigens presented by local APCs. Intimately involved in both migration and activation of T cells in the CNS are adhesion and costimulatory molecules expressed on vascular endothelial cells and APCs, respectively, as well as chemokines and cytokines released in response to inflammatory stimuli (4–6). The expression of these cell surface molecules and cytokines in the CNS is tightly regulated due to a limited capacity for CNS self-regeneration. Among the soluble mediators regulating the expression of these molecules is a 12.5-kDa protein known as macrophage migration inhibitory factor (MIF). MIF was one of the first cytokines described, and is secreted by activated T cells, macrophages, and a variety of nonimmune cells (7–10). MIF was recently cloned and shown to have a plethora of immunologic activities, including the inhibition of migration and enhanced TNF-α and NO production by macrophages (11, 12). Furthermore, it regulates T cell activation and proliferation (13). Recently, MIF has been implicated in the pathogenesis of autoimmune disorders such as arthritis, glomerulonephritis, and lupus (14–16). Moreover, elevated levels of MIF were reported in the cerebrospinal fluid of patients with MS (17). MIF is constitutively expressed in the CNS, and it is up-regulated in response to inflammatory and infectious stimuli (18, 19). However, very little is known about the role of MIF in the regulation of T cell responses in the CNS, and no direct evidence has been provided for its involvement in the pathogenesis of MS/experimental autoimmune encephalomyelitis (EAE).

In this study, we show for the first time that treatment with anti-MIF Abs reduces the severity of acute EAE in mice and accelerates recovery from disease. The results show that MIF blockade decreases the expression of VCAM-1 in the CNS, and impairs the homing of neuroantigen-specific T cells to this site. Moreover, MIF blockade reduces the clonal size of the autoantigen-specific Th1 cells, and increases their activation threshold.

Materials and Methods

Animals, Ags, and treatments

Mice were purchased from The Jackson Laboratory (Bar Harbor, ME) and maintained at Case Western Reserve University under specific pathogen-free conditions. All animal procedures were conducted according to guidelines of the Institutional Care and Use Committee of Case Western Reserve University. Female SJL/J and C57BL/6 mice were injected at 6–10 wk of age with the Ags (listed in this section) in CFA. Pertussis toxin (PT; 200 ng; List Biological Laboratories, Campbell, CA) was injected i.p. in 500 μl of saline at 0 and 24 h after injection as indicated in the legend to Fig. 1. PLP peptide aa 139–151 ($PLP_{139-151}$; HSLGKWLGHPDKF) was synthesized by Princeton Biomolecules (Langhorne, PA). IFA was purchased from Life Technologies (Grand Island, NY), and CFA was made by mixing *Mycobacterium tuberculosis* H 37 Ra (Difco Laboratories, Detroit, MI) at 5 mg/ml into IFA. Ags were mixed with the adjuvant to yield a 2 mg/ml emulsion, of which 50 μl was injected s.c. Neutralizing anti-MIF mAb

*Institute of Pathology, School of Medicine, Case Western Reserve University, and †Department of Medicine, University Hospitals of Cleveland, Cleveland, OH 44106; ‡Institute of Virology and Immunology, University of Würzburg, Würzburg, Germany; and §Picower Institute for Medical Research, Manhasset, NY 11030

Received for publication June 28, 2002. Accepted for publication November 15, 2002.

The costs of publication of this article were defrayed in part by the payment of page charges. This article must therefore be hereby marked *advertisement* in accordance with 18 U.S.C. Section 1734 solely to indicate this fact.

[1] This work was supported by National Institutes of Health Grants AI-41609-01 and 1RO1AR45918, and the Harry Weaver Neuroscience Scholarship JF-2092-A-1 from the National Multiple Sclerosis Society (to T.G.F.), and a fellowship of the Studienstiftung der Deutschen Wirtschaft and the Boehringer Ingelheim Fond (to C.M.D.).

[2] Address correspondence and reprint requests to Dr. Thomas G. Forsthuber, Institute of Pathology, School of Medicine, Case Western Reserve University, Biomedical Research Building 936, 2109 Adelbert Road, Cleveland, OH 44106-4943. E-mail address: tgf2@pop.cwru.edu

[3] Abbreviations used in this paper: MS, multiple sclerosis; MIF, macrophage migration inhibitory factor; EAE, experimental autoimmune encephalomyelitis; PT, pertussis toxin; PLP, proteolipid protein; VLA-4, very late Ag 4; IP-10, IFN-γ-inducible protein-10; MIP-1α, macrophage-inflammatory protein-1α; MCP-1, monocyte chemoattractant protein-1.

0022-1767/03/$02.00

(clone XIV.15.5, IgG1 isotype) was prepared as previously described (20). The isotype matched control mAb (IgG1) was purified similarly using the hybridoma 5D4-11 (HB-49; American Type Culture Collection, Manassas, VA). The Abs were injected i.p. at 0.5 mg/mouse in 0.5 ml of saline as indicated in the figures.

Evaluation of clinical disease in mice

Mice were monitored daily after injection of neuroantigen, and the severity of disease was recorded according to the following scale (21): grade 0, no abnormality; grade 1, limp tail; grade 2, moderate hind limb weakness; grade 3, complete hind limb paralysis; grade 4, quadriplegia or premoribund state; and grade 5, death. If necessary, food was provided on the cage floor. Where indicated, statistical analysis was performed using the paired *t* test, comparing the mean EAE grade of all mice in one group with that of the other group at different time points.

Cell preparations from the organs tested and adoptive transfer

Single-cell suspensions from the spleen were prepared as previously described (22). The cells were counted and plated with Ag in HL-1 serum-free medium (BioWhittaker, Walkersville, MD) at 1×10^6 cells/well, and tested as indicated in Fig. 5. For adoptive transfer experiments, splenic mononuclear cells from mice immunized as indicated in the figures were prepared as described (22). These cells were subsequently preactivated by incubation with $PLP_{139-151}$ at the previously established optimal stimulatory concentration (20 μg/ml) in complete DMEM for 4 days before i.p. injection into the recipient animals.

Cytokine measurements by ELISPOT and computer-assisted ELISPOT image analysis

The ELISPOT assay was performed as described previously (23). Briefly, ELISPOT plates (ImmunoSpot; Cellular Technology, Cleveland, OH) were coated overnight with IFN-γ (R46A2; 4 μg/ml), IL-2 (JES6-1A12; 2 μg/ml), IL-3 (MP2-8F8; 4 μg/ml), IL-4 (BVD4-1D11; 4 μg/ml), or IL-5 (TRFK5; 5 μg/ml) specific capture Ab. The plates were blocked with 1% BSA in PBS for 1 h at room temperature, and then washed four times with PBS. Spleen cells were plated at 10^6 cells/well alone or with Ag (7 μM) in HL-1 medium and cultured for 24 h for IFN-γ, IL-2, or IL-3, or 48 h for IL-4 or IL-5. Subsequently, the cells were removed by washing and the biotinylated detection Ab XMG1.2-biotin (2 μg/ml) for IFN-γ, JES6-5H4-biotin (0.25 μg/ml) for IL-2, MP2-43D11 (0.5 μg/ml) for IL-3, BVD6-2462 (0.2 μg/ml) for IL-4, and TRFK4-biotin (2 μg/ml) for IL-5 were added and incubated overnight. The plate-bound second Ab was then visualized by adding streptavidin-alkaline phosphatase (SAV-AP; DAKO, Carpinteria, CA) and nitroblue tetrazolium/5-bromo-4-chloro-3-indolyl phosphate substrate (Bio-Rad, Hercules, CA; Sigma-Aldrich, St. Louis, MO). Image analysis of ELISPOT assays was performed on a Series 1 ImmunoSpot Image Analyzer (Cellular Technology) as described previously (24, 25). In brief, digitized images of individual wells of the ELISPOT plates were analyzed for cytokine spots, based on the comparison of experimental (containing T cells and APC with Ag) and control wells (T cells and APC, no Ag). After separation of spots that touched or partially overlapped, nonspecific noise was gated out by applying spot size and circularity analysis as additional criteria. Spots that fell within the accepted criteria were highlighted and counted. The stimulation index was calculated by dividing the number of cytokine spots detected in wells pulsed with cognate Ag by the number of cytokine spots in wells without Ag (medium only). The spot number in unimmunized or control mice (irrelevant Ag) was in the same range as that of the medium controls. Where indicated, statistical analysis was performed using the paired *t* test, χ^2 test, or the Mann-Whitney rank sum test using SigmaStat software (SPSS, Chicago, IL).

Flow cytometry analysis for expression of surface molecules (CD3, CD4, CD19, and CD11b)

Single-cell suspensions of spinal cord isolates were incubated at 1×10^6 cells/sample with 1 μg of the respective FITC- or PE-labeled anti-mouse Abs (BD PharMingen, San Diego, CA) in PBS for 1 h on ice. Cells were washed with PBS and erythrocytes were lysed with Immuno-lyse (Coulter, Miami, FL). The cells were then fixed in Coulter Clone fixative reagent and read on a BD Biosciences FACScan flow cytometer. The flow cytometry data was analyzed using CellQuest software (BD Biosciences).

Histopathology, immunofluorescence staining, and cell counting

At the time of the experiment, the brain and spinal cord of the mice were removed and either preserved in 10% formalin or snap-frozen in 2-methylbutane. Five-micrometer slices of the CNS tissue were prepared and stained with H&E. The tissue was then examined by light microscopy in a blinded fashion by a pathologist and evaluated for the extent of inflammation and graded as follows: −, no inflammation; +/−, a few mononuclear cells; +, organization of inflammatory infiltrates around positive vessels; ++, extensive perivascular cuffing with extension into the subarachnoid space; and +++, extensive perivascular cuffing with increasing subarachnoid inflammation (21, 26). Immunofluorescence staining of the brain tissue was performed as described (27). In brief, 5-μm sections of snap-frozen brain tissue were fixed with 4% paraformaldehyde and probed with FITC- or PE-conjugated anti-mouse-CD3, -CD4, -CD19, -MAC-1, and -F4/80 Abs (BD PharMingen). Images of Ab-labeled tissue sections were captured using a Leica fluorescence microscope equipped with a CCD camera at ×400 magnification, and image analysis software (Spot 2.0; Diagnostic Instruments, Sterling Heights, MI). Sections were blindly analyzed by two experienced observers as follows: immunostained T cells (CD3), B cells (CD19), and macrophages/microglia (MAC-1, F4/80) were counted on four sections obtained in a standardized fashion from different levels of the neuraxis. On each slide, four inflammatory foci (meningeal, perivascular, between two lobes, and in the gray matter) were selected and scored for the number of cells staining positively for the respective markers. The result was calculated as the mean ± SD of numbers of cells in each category over all lesions counted.

Evaluation of staining intensity

Evaluation of expression of adhesion molecules on brain vessels was performed on CNS tissue sections as described (28) with FITC- or PE-labeled monoclonal VCAM-1 or ICAM-1 Abs (BD PharMingen). Briefly, after immunofluorescence staining for ICAM-1 and VCAM-1, images of brain vessels were captured at ×400 with a Leica fluorescence microscope equipped with a CCD camera and image analysis software (Diagnostic Instruments). For the evaluation of the relative fluorescence intensity, the mean brightness value of the green (FITC) or red (PE) fluorescence channel of the three most intensely stained areas of the vessel was determined using Adobe Photoshop 6.0 (Adobe Systems, San Jose, CA) with a set 200-pixel square area. The background reading in unstained areas was subtracted from these values. Four sections from different levels of the neuraxis were taken. Four vessels from each section were analyzed and the mean ± SEM of the fluorescence intensity for each group of mice was calculated.

Results

Anti-MIF Ab treatment reduces EAE severity, duration, and CNS pathology

The role of MIF in the pathogenesis of EAE has not been studied. To address this question, we induced EAE in SJL/J mice by immunization with the immunodominant H-2^s-restricted PLP peptide $PLP_{139-151}$. Subsequently, the mice were randomized into two groups and injected with either anti-MIF or isotype-matched control Abs every other day for 2 wk. The anti-MIF Ab treatment was initiated 6 days after immunization with the PLP peptide because we reasoned that the $PLP_{139-151}$-specific T cells were already primed at this time point, and treatment with anti-MIF Abs would therefore elucidate whether or not MIF was required for the induction of EAE by these cells in the CNS.

Interestingly, as shown in Fig. 1*a*, the injection of anti-MIF Abs significantly reduced clinical EAE symptoms. As shown in Table I, the incidence and mean EAE score of anti-MIF Ab-treated mice were significantly lower as compared with those of control Ab-injected animals (incidence 81.8 vs 100%, respectively; mean EAE score of 2.7 ± 0.2 vs 3.9 ± 0.2), and the disease duration was shorter (7.0 ± 0.7 days vs 10.0 ± 0.4 days, respectively). Moreover, the lethality was significantly decreased (21.2 vs 48.5%, respectively). Hence, the data showed that the treatment was effective when the anti-MIF Abs were injected before the onset of disease.

However, in human MS patients, treatment can begin only after the onset of the disease symptoms. Therefore, we asked whether or not anti-MIF Ab treatment was also efficacious after the onset of

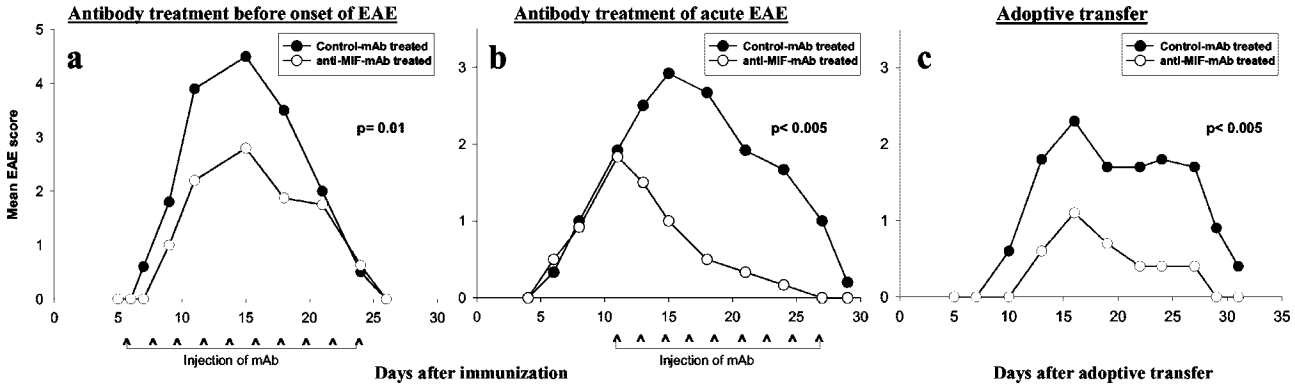

FIGURE 1. Anti-MIF Ab treatment improves EAE. *a*, Six- to 8-wk-old SJL/J mice were immunized with $PLP_{139-151}$ in CFA and PT. Mice were randomly assigned into two groups and Abs were injected i.p. every second day before the onset of disease as indicated (∧) on day 6 after immunization. *b*, EAE was induced as above. Mice were observed for clinical signs of EAE and then randomly assigned to either the anti-MIF Ab-treated group (○) or the control Ab-treated group (●). The Abs were injected i.p. every second day after onset of disease as indicated (∧) on day 11 after immunization. *c*, Groups of SJL/J mice ($n = 10$ per group) were injected with anti-MIF or control Ab every second day for 5 days. Two days after the last injection, the mice from both groups were adoptively transferred with 50×10^6 preactivated $PLP_{139-151}$-specific T cells (short-term T cell lines generated in the absence of Abs) and observed for EAE symptoms. Experiments were performed as outlined in *Materials and Methods*. Shown are the mean EAE scores for one representative experiment ($n = 6–10$ mice per group) repeated two to four times with similar results.

EAE symptoms. For this, EAE was induced in SJL mice by immunization with the $PLP_{139-151}$ peptide as outlined above. As shown in Fig. 1*b*, all of the mice developed clinical EAE symptoms by day 9. The mice were then randomized into two groups and injected with either anti-MIF or control Ab starting on day 11 after immunization, i.e., at a time when the disease began to peak. Importantly, the disease symptoms improved rapidly in the anti-MIF Ab-injected mice (Fig. 1b, ○ vs ●), and most of the animals recovered completely within 3–4 days. In strong contrast, EAE symptoms continued to worsen in the control Ab-treated mice, and they recovered significantly later (mean EAE scores 2.6 ± 0.2 in the control mice vs 1.6 ± 0.2 in the anti-MIF Ab-treated mice; disease duration 14.9 ± 1.3 vs 8.7 ± 1.1 days). To delineate anti-MIF Ab effects on the afferent or efferent phase of the autoimmune response in this model, we performed adoptive transfer experiments. As shown in Fig. 1*c*, groups of naive SJL mice were treated with anti-MIF Abs (○) or control Abs (●). Two days after the last injection, the same number of activated $PLP_{139-151}$-reactive T cells (short-term T cell lines generated in the absence of control or anti-MIF Abs) was adoptively transferred into both groups. The data show that the pretreatment of the recipients with anti-MIF Abs ameliorated the EAE course (statistically significant, $p < 0.005$). Moreover, the disease onset in anti-MIF Ab-treated mice was significantly delayed (day 12 for anti-MIF-treated mice vs day 6 for control Ab-treated mice). Hence, the data indicate that the anti-MIF treatment affected the efferent phase of the autoimmune response.

The amelioration of clinical EAE symptoms in anti-MIF Ab-treated mice was reflected by the reduced CNS pathology. As shown in Fig. 2, *a* and *b*, control Ab-treated mice with actively induced EAE showed extensive perivascular and periventricular inflammation, and the inflammatory infiltrates extended into the CNS parenchyma. The inflammatory cells consisted mainly of $CD4^+$ T lymphocytes and macrophages/microglia (Fig. 2*c*). In contrast, anti-MIF Ab-treated mice showed significantly less CNS inflammation, and the infiltrates remained localized to the perivascular space without significant parenchymal infiltration (Fig. 2, *d–f*). Similar histologic findings were obtained when the treatment was initiated on day 6, i.e., before the onset of EAE (not shown).

Taken together, the results showed that the anti-MIF Ab treatment ameliorated EAE and reduced disease severity, duration, and CNS pathology. Moreover, the MIF blockade was efficacious for the treatment of acute EAE in mice after the onset of disease symptoms.

Several mechanisms could account for the observed effects of anti-MIF Ab treatment on EAE. First, the Ab treatment could inhibit the recruitment of activated neuroantigen-reactive T cells to the CNS. Second, MIF blockade could affect the priming, clonal expansion, and/or the effector functions of neuroantigen-reactive T cells. Third, MIF immunoneutralization could impair APC effector functions in the CNS, and finally, the treatment could trigger immunoregulatory mechanisms, such as regulatory T cells.

Treatment with anti-MIF Abs impairs T cell migration to the CNS

MIF has been reported to regulate the expression of molecules such as chemokines, chemokine receptors, or adhesion molecules involved in the migration of T cells to sites of inflammation (4–6). Consistent with these reports, we noted a decrease in inflammatory cells in the CNS of anti-MIF Ab-treated mice with EAE (Fig. 2, *d–f*). Hence, to test the hypothesis that anti-MIF Ab treatment impaired the migration of pathogenic T cells to the CNS, we quantified the number of $CD3^+CD4^+$ T cells, B cells, and macrophages

Table I. *Effect of anti-MIF mAb treatment on the development of EAE*[a]

Treatment	Incidence (%)	Onset (day)	Duration (days)	Clinical Score	Lethality (%)
Control mAb	100.0 (33/33)	10.0 ± 0.4	10.0 ± 0.4	3.9 ± 0.2	48.5 (16/33)
Anti-MIF mAb	81.8 (27/33)	11.1 ± 0.3	7.0 ± 0.7	2.7 ± 0.2	21.2 (7/33)
	($p < 0.03$)	($p > 0.05$)	($p < 0.001$)	($p < 0.001$)	($p < 0.05$)

[a] Mice were immunized with 50 μg of $PLP_{139-151}$/CFA (s.c.) plus PT (i.p.) and assessed for disease in a blinded fashion as outlined in *Materials and Methods.* Anti-MIF mAb or control mAb was injected i.p. every other day starting on day 6. The data were obtained in four independent experiments ($n = 6–10$ mice per group for each experiment). The results for each independent experiment were statistically significant.

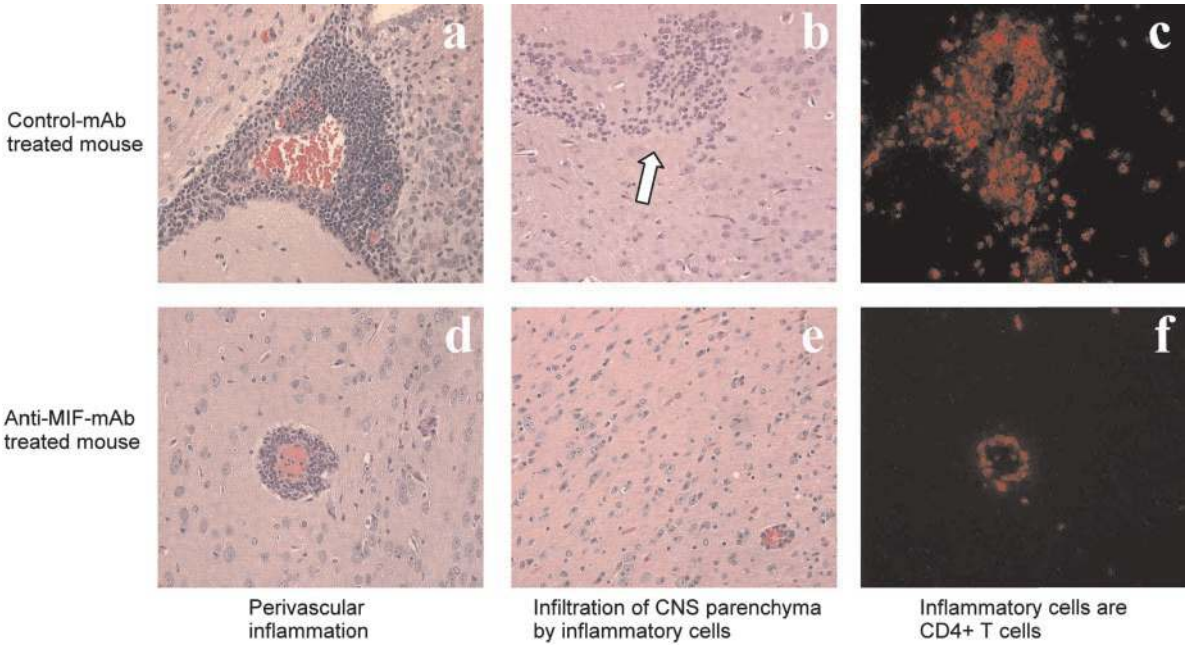

FIGURE 2. Anti-MIF Ab treatment ameliorates CNS pathology. Histologic analysis of H&E-stained brain sections of representative SJL/J mice with acute EAE treated with control (*a–c*) or anti-MIF Abs (*d–f*), starting on day 11 after immunization, was performed as outlined in *Materials and Methods* (sections obtained on day 14). Control Ab-injected SJL mice with EAE show extensive perivascular inflammation (*a*) with infiltration into the CNS parenchyma (*b*). *c*, Immunofluorescence staining demonstrating $CD4^+$ T cells in the CNS parenchyma. MAC-1^+ cells, but not $CD19^+$ B cells (not shown), were present. Anti-MIF Ab-injected mice show significantly less perivascular inflammation and no infiltration of inflammatory cells into the parenchyma (*d–f*). Similar results were obtained in four independent experiments.

in the CNS of anti-MIF or control Ab-treated mice with EAE by immunofluorescence staining and flow cytometry. As shown in Fig. 3, *a* and *b*, the number of $CD3^+CD4^+$ T cells was significantly decreased in the CNS of anti-MIF Ab-treated mice as compared with that of control Ab-injected animals ($p < 0.02$). However, no significant difference was noted between the two groups in the number of macrophages/microglia ($p > 0.05$). The number of B cells was below the detection limit. Importantly, the absolute number of cells and the percentage of T cells, B cells, or macrophages in the spleens of anti-MIF or control Ab-treated mice were similar (not shown), indicating that the results were not due to an overall reduction of $CD4^+$ T cells by the Ab treatment. Similar results were obtained when the Ab treatment was initiated on day 11 after immunization (not shown), and in studies in which we induced EAE in C57BL/6 mice with myelin oligodendrocyte glycoprotein peptide 35–55 and treated with anti-MIF or control Abs. Hence, the data show that the effects of MIF blockade on EAE are strain- and neuroantigen-independent (data not shown).

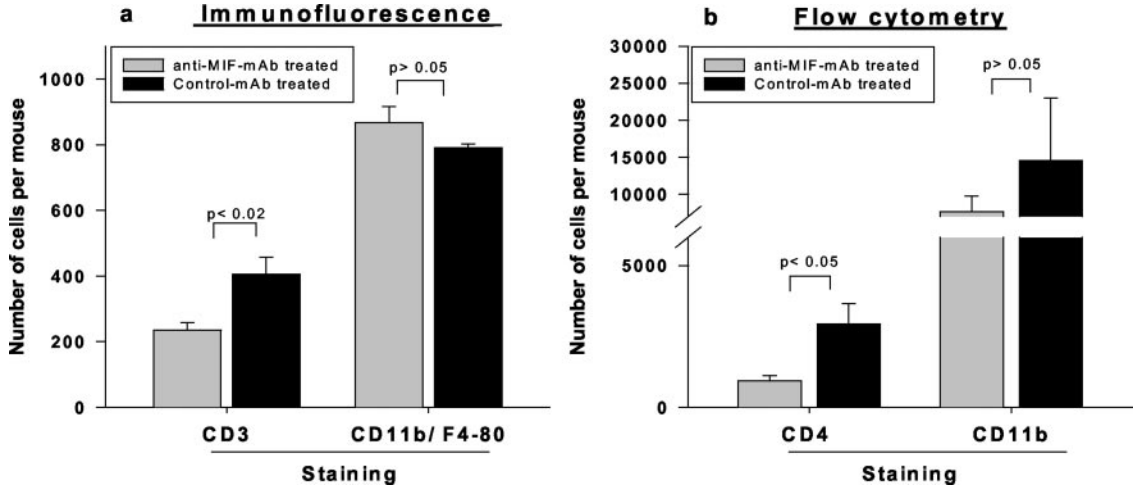

FIGURE 3. Anti-MIF Ab treatment impairs the migration of $CD3^+CD4^+$ T cells to the CNS. Six- to 8-wk-old SJL/J mice were immunized with $PLP_{139-151}$ in CFA and PT. Mice were observed for clinical signs of EAE and randomly assigned to either the anti-MIF Ab-treated group (▨) or the control Ab-treated group (■). The Abs were injected i.p. every second day starting on day 6. The brains of the mice were removed after 3 wk and stained with monoclonal anti-CD3, -CD4, -CD19, -CD11b, or -F4/80 Abs. *a*, Shown are the mean ± SD of the number of cells per brain staining positive for CD3 or CD11b/F4/80 by immunofluorescence histology averaged over four areas for four sections of the brain ($n = 10$ mice per group). *b*, Shown are the mean ± SD of the number of CD4- or CD11b-positive cells per 5×10^5 spinal cord cells measured by flow cytometry ($n = 10$ mice per group). Experiments were performed as outlined in *Materials and Methods*. Similar results were obtained in three independent experiments.

To conclude, the results showed that anti-MIF Ab treatment decreased the inflammatory $CD4^+$ T cell infiltrates in the CNS of mice with EAE. Moreover, the data suggested that the mechanism underlying the efficacy of anti-MIF Ab treatment in EAE involved an impaired migration of encephalitogenic T cells to the CNS.

Treatment with anti-MIF Abs decreases the expression of VCAM-1 in the CNS of mice with EAE

The migration of encephalitogenic T cells to the CNS is dependent on the interaction of adhesion molecules, such as very late Ag 4 (VLA-4) on T cells, with VCAM-1 expressed by vascular endothelial cells (4, 29, 30). Therefore, we investigated whether or not the impaired CNS homing of T cells in anti-MIF Ab-treated mice was associated with an altered expression of VCAM-1 or ICAM-1, two of the adhesion molecules implicated in the migration of T cells into the brain.

Interestingly, as shown in Fig. 4, anti-MIF Ab treatment decreased the expression of VCAM-1 on vascular endothelial cells in the CNS, as compared with the control Ab-injected animals (Fig. 4*a*, *left* ▨ vs *left* ■, $p < 0.005$; Fig. 4*b*, *bottom left* vs *top left*). By contrast, there was no significant difference in the expression of ICAM-1 in both groups (Fig. 4*a*, *right* ▨ vs *right* ■, $p > 0.05$; Fig. 4*b*, *bottom right* vs *top right*, staining indicated by arrows). Double staining with VCAM-1 and CD31 (platelet endothelial cell adhesion molecule-1) confirmed that VCAM-1 was expressed on endothelial cells (not shown). Furthermore, the levels of CD31 expressed in the CNS of anti-MIF or control Ab-treated mice were similar (not shown), arguing against a significant role for this molecule in the amelioration of EAE in this model.

Together, the data showed that anti-MIF Ab treatment decreased the expression of VCAM-1 in the brain. Furthermore, the results implicated decreased expression of VCAM-1 as the mechanism responsible for the decreased homing of T cells to the CNS in this study.

The frequencies of $PLP_{139-151}$-reactive Th1 cells are decreased in the CNS of anti-MIF Ab-treated mice

Our results suggested that anti-MIF Ab treatment impaired the homing of T cells to the CNS during EAE. However, the Ab treatment could selectively affect the CNS homing of encephalitogenic $PLP_{139-151}$-specific T cells, and/or it could prevent the migration of bystander T cells to this site. Moreover, the treatment could impair the survival of neuroantigen-specific T cells in the CNS. To directly address these questions, we measured the frequencies and cytokine profiles of $PLP_{139-151}$-reactive T cells in the CNS at single-cell resolution by computer-assisted cytokine ELISPOT assay. Shown in Fig. 5*a* are the results of $PLP_{139-151}$-immunized SJL mice treated with the anti-MIF Ab during acute EAE (day 11, ▨) or control Ab (■). Recall assays with the cognate Ag were performed 2 wk after immunization. Interestingly, the frequencies of $PLP_{139-151}$-reactive IFN-γ-secreting Th1 cells in the CNS were significantly reduced in anti-MIF Ab-treated mice, as compared with the control group ($p < 0.001$). Moreover, the data show that the anti-MIF Ab treatment at this time point did not affect the priming of these T cells, because high frequencies of $PLP_{139-151}$-reactive T cells could be detected in the spleen of these mice (Fig. 5*b*). Furthermore, there was no bias toward IL-5 (Fig. 5, *a* and *b*,

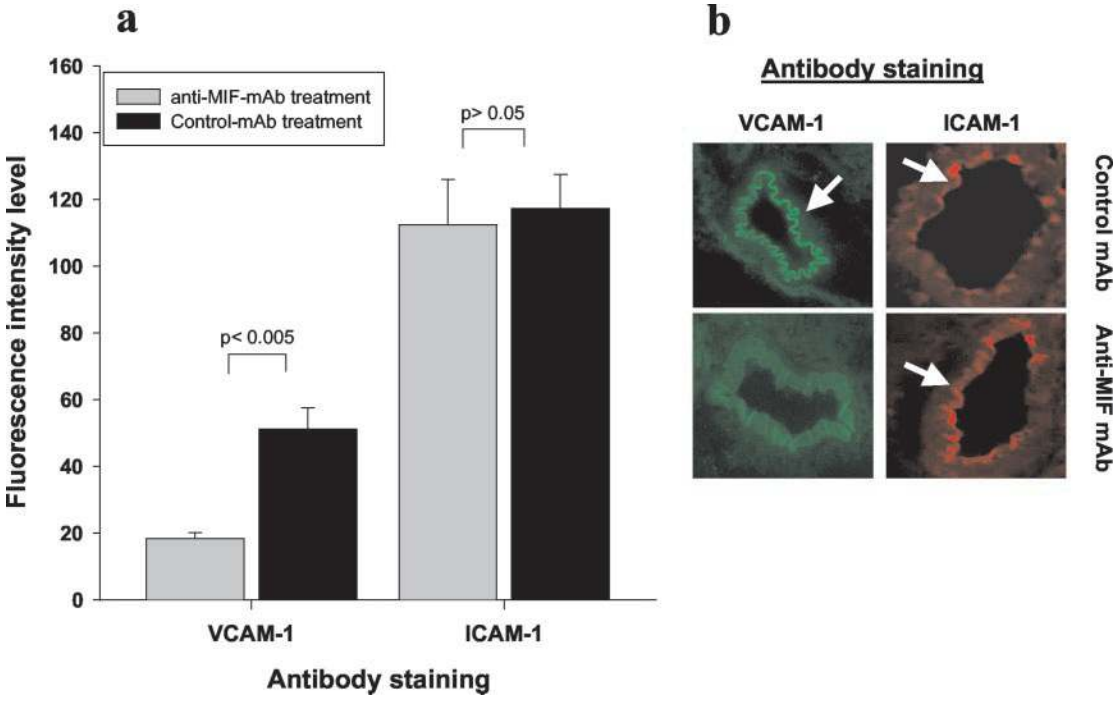

FIGURE 4. Anti-MIF Ab treatment decreases the expression of VCAM-1 in the CNS. Six- to 8-wk-old SJL/J mice were immunized with $PLP_{139-151}$ in CFA and PT. Mice were observed for clinical signs of EAE, and randomly assigned to either the anti-MIF Ab-treated group (▨) or the control Ab-treated group (■). The Abs were injected i.p. every second day starting from day 6. The brains of the mice were removed after 3 wk and stained with monoclonal VCAM-1 or ICAM-1 Abs. The relative fluorescence intensity of the three most intensely stained areas of the vessels was determined by digital image analysis as outlined in *Materials and Methods*. *a*, Shown are the results of the immunofluorescence staining of the brains showing the mean fluorescence intensity ± SEM averaged over four vessels per each of four sections per brain, averaged over 10 mice per group. Similar results were seen in three independent experiments. *b*, Shown are representative sections of anti-MIF (*bottom*) or control Ab-treated mice (*top*) stained with VCAM-1 (*left*) or ICAM-1 (*right*). Staining for the adhesion molecules on the endothelium is indicated by arrows. Expression of VCAM-1 on endothelial cells was confirmed by double staining with CD31 (not shown).

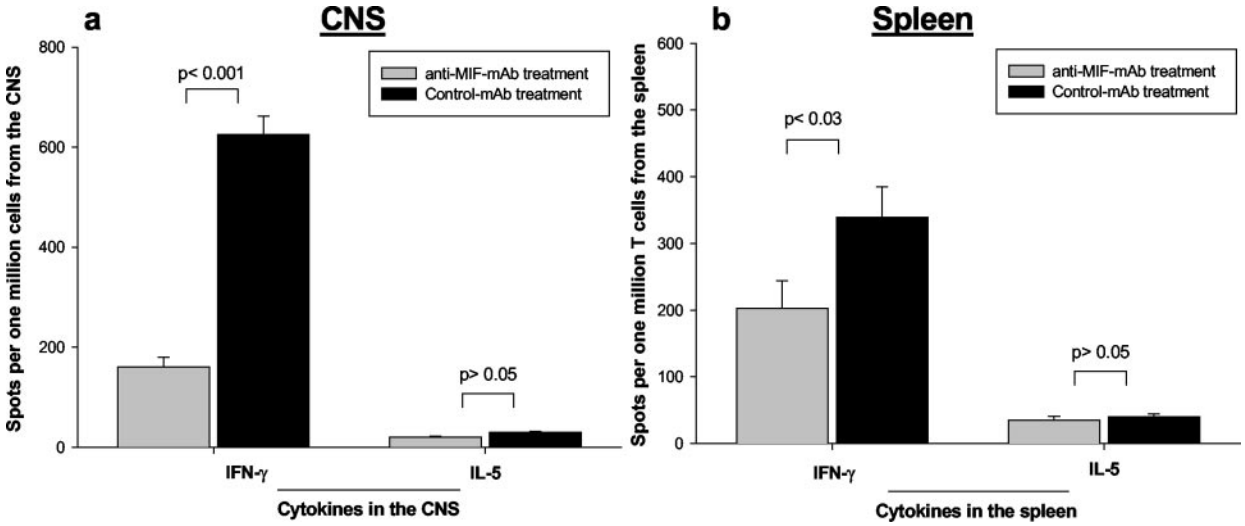

FIGURE 5. Anti-MIF Ab decreases the frequencies of neuroantigen-reactive Th1 cells in the CNS. Six- to 8-wk-old SJL/J mice were immunized with $PLP_{139-151}$ in CFA and PT. Mice were randomly assigned to either the anti-MIF Ab-treated group (▨), or the control Ab-treated group (■). Starting on day 11 after immunization, the Abs were injected i.p. every second day. The frequencies of $PLP_{139-151}$-specific IFN-γ- and IL-5-producing T cells were measured after 3 wk by cytokine ELISPOT assay in single-cell suspensions of CNS isolates (*a*) or $CD4^+$ T cells purified from the spleen (*b*) as described in *Materials and Methods*. Shown are the numbers of cytokine-producing cells per million cells. Shown are the results of groups of six mice, and the values shown are the means ± SD of triplicate wells, with the background subtracted (usually less than five spots). Stimulation index of >3 is considered positive (see *Materials and Methods*). Similar results were obtained in three independent experiments with Ab treatment starting on day 11, and in two independent experiments with Ab treatment starting on day 6.

right bars) or IL-4/IL-10 production (not shown), arguing against the induction of protective $PLP_{139-151}$-specific Th2 immunity.

To test whether or not the survival of the T cells in the CNS of the anti-MIF-treated mice was affected, we tested the degree of T cell apoptosis in the CNS. Interestingly, sections from the brains of anti-MIF Ab-treated mice stained by TUNEL technique showed an increase in the number of apoptotic T lymphocytes as compared with those of control Ab-injected mice (data not shown), suggesting that MIF blockade rendered activated neuroantigen-specific T cells more susceptible to in situ apoptosis.

To summarize, the results indicated that the anti-MIF Ab treatment selectively decreased the frequencies of $PLP_{139-151}$-specific T cells in the CNS. Moreover, the results suggested that, in addition to their impaired homing, the survival of $PLP_{139-151}$-reactive T cells in the CNS was impaired.

The activation threshold of $PLP_{139-151}$-reactive T cells is increased in anti-MIF Ab-treated mice with EAE

Treatment of EAE with anti-MIF Abs ameliorated disease and decreased the frequencies of $PLP_{139-151}$-reactive T cells in the CNS and the spleen. However, in addition, the function of these T cells could have been affected by the treatment. Therefore, we tested the cytokine production of $PLP_{139-151}$-specific T cells from anti-MIF or control Ab-treated SJL mice as a function of Ag concentration in cytokine ELISPOT recall assays. As shown in Fig. 6, the activation of T cells (production of IFN-γ) recovered from the CNS of anti-MIF Ab-treated mice required 10- to 100-fold higher concentrations of PLP peptide as compared with T cells from control Ab-injected mice (Fig. 6*a*, ▨ vs ■, respectively). Similar results were obtained when purified $CD4^+$ T cells from the spleens of both groups were tested with irradiated APCs from untreated naive SJL mice (Fig. 6*b*, ▨ vs ■, respectively), indicating that the observed differences were primarily the result of a change in the T cell compartment. Moreover, adoptive-transfer experiments showed that $PLP_{139-151}$-reactive T cells derived from anti-MIF Ab-treated mice were less pathogenic than were cells from control Ab-treated mice (data not shown).

Taken together, the data show that T cells from anti-MIF Ab-treated mice have an increased activation threshold for stimulation with the $PLP_{139-151}$ peptide, as compared with T cells from control Ab-treated mice. The results suggested that the loss of $PLP_{139-151}$-reactive T cells with a high functional avidity could be due to the observed increase in apoptosis in the CNS of anti-MIF Ab-treated mice.

Discussion

In this study, we show for the first time that anti-MIF Abs are highly effective in the treatment of acute EAE. The results indicate that MIF blockade impairs the migration of neuroantigen-reactive T cells to the CNS and decreases their clonal size, while increasing their activation threshold.

The migration of autoreactive T cells to sites of the autoimmune attack is critically dependent on the interaction of adhesion molecules on these cells with their ligands such as VCAM-1, ICAM-1, CD31, and LFA-1 on tissues in the target organ (31–35). Thus, the delayed onset and reduced severity of EAE in anti-MIF-treated mice appeared to be the consequence of the decreased expression of VCAM-1 in the CNS. This interpretation is consistent with reports demonstrating that anti-MIF Ab treatment prevented the up-regulation of VCAM-1 and ameliorated disease in a glomerulonephritis model in rats (36). Similarly, VCAM-1 and VLA-4, its ligand expressed on T cells, have been linked to the ability of neuroantigen-reactive T cells to migrate to the CNS and cause EAE (31). However, in contrast to these results, application of anti-VLA-4 Abs prevented or ameliorated EAE only if it was initiated before the onset of disease (37). Moreover, treatment with anti-VLA-4 Abs during acute disease exacerbated EAE and enhanced the accumulation of T cells in the CNS, which produced higher levels of IFN-γ and IL-2.

Hence, the therapeutic efficacy of anti-MIF Abs during acute EAE may not be only the result of impaired homing of T cells to the CNS due to the down-regulation of VCAM-1. MIF blockade may, in addition, impair the effector functions of T cells and/or microglia/oligodendrocytes, such as the production of cytokines or chemokines. In particular, IFN-γ-inducible protein-10 (IP-10;

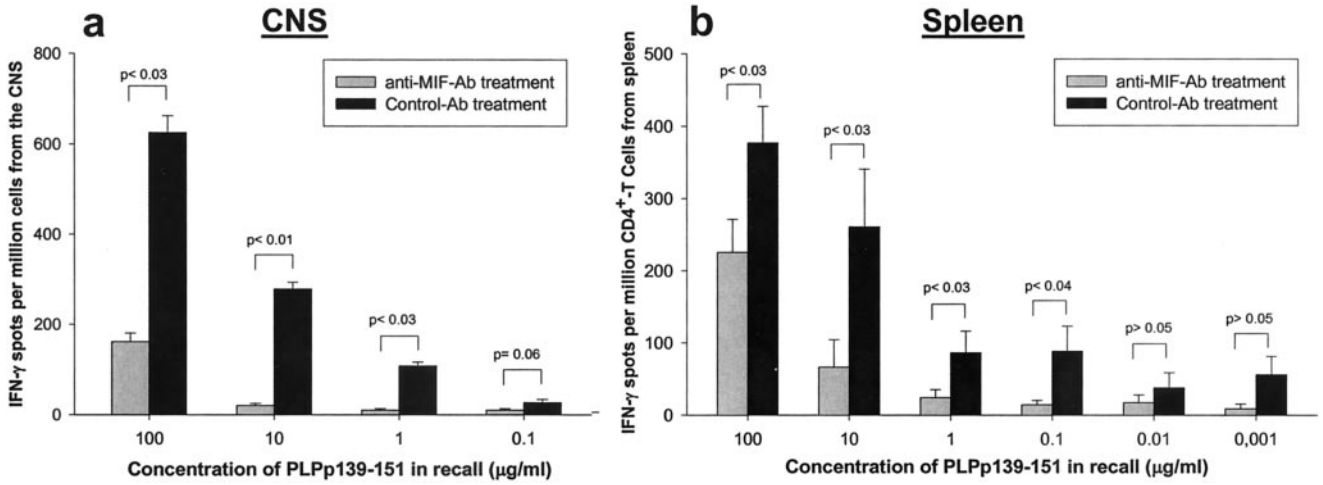

FIGURE 6. The activation threshold of $PLP_{139-151}$-reactive T cells is increased in anti-MIF Ab-treated mice. Six- to 8-wk-old SJL/J mice were immunized with $PLP_{139-151}$ in CFA and PT. Mice were randomly assigned to either the anti-MIF Ab-treated group (▨) or the control Ab-treated group (■), and treatment was started on day 11 with the Abs injected i.p. every second day. The frequencies of $PLP_{139-151}$-specific IFN-γ-producing T cells in single-cell suspensions of CNS isolates (*a*) or $CD4^+$ T cells purified from the spleens (*b*) were measured after 3 wk by cytokine ELISPOT assay in single-cell suspensions of spleen cells as described in *Materials and Methods* with the cognate Ag titrated as indicated on the *x*-axis. Shown are means ± SD of cytokine-producing cells per million spleen cells for groups of eight mice as outlined in *Materials and Methods*. Similar results were obtained in three independent experiments.

CXCL10), macrophage-inflammatory protein-1α (MIP-1α), and monocyte chemoattractant protein-1 (MCP-1) have been implicated in the migration of activated T cells into the CNS during EAE (38–40). Treatment with anti-MIP-1α prevented acute EAE (5), whereas anti-MCP-1 treatment decreased the severity of clinical relapses (41). IP-10-deficient mice showed decreased recruitment of $CD4^+$ and $CD8^+$ T cells into the brain in combination with reduced levels of demyelination upon infection with a neurotropic mouse hepatitis virus, suggesting a role for IP-10 in regulating T cell trafficking into the CNS in vivo (42). Furthermore, MIF induced IL-8 in monocytes and dendritic cells (43), and anti-MIF Ab treatment inhibited MCP-1-induced chemotaxis of human PBMCs (44), indicating a role for MIF in the regulation of chemokine expression. However, we are not aware of direct effects of MIF on IP-10 or MIP-1α, i.e., chemokines relevant to the acute phase of disease that we have investigated. Moreover, we consider it unlikely that the enhanced activation threshold of PLP-specific T cells that we have observed was due to altered levels of chemokines in the CNS, because anti-IP-10 treatment did not affect the activation or pathogenic potential of encephalitogenic T cells (39). In contrast, the reduced expression of VCAM-1 could impair the homing of these cells to the brain, and, in addition, decrease their survival via the deprivation from antiapoptotic signals (45). Consistent with an additional role for MIF in the survival of autoreactive T cells in the CNS in EAE, we found that anti-MIF Ab treatment dramatically decreased the frequencies of IFN-γ-producing $PLP_{139-151}$-reactive Th1 cells in the CNS, whereas the frequencies in the spleen were only moderately reduced. Moreover, the activation threshold of PLP-reactive T cells in anti-MIF Ab-treated mice was significantly decreased, suggesting that the treatment affected T cells with high affinity for self-Ag (46). Because MIF has been reported to be important for the priming and activation of T cells (13), impaired recruitment of naive T cells into the effector/memory T cell pool could have contributed to the observed reduction in the frequencies of PLP-reactive T cells. However, the dramatic decrease in $PLP_{139-151}$-reactive T cells in the CNS was also seen when the anti-MIF Ab treatment was started on day 6 or day 11 after immunization, i.e., at a time point when the majority of PLP-specific T cells was already primed. Moreover, we found that anti-MIF treatment significantly ameliorated EAE and delayed the onset of disease symptoms upon adoptive transfer of activated PLP-reactive T cells. Thus, while impaired priming of naive T cells may have contributed to the lower frequencies of neuroantigen-specific T cells, overall the data show that MIF blockade was dominant in its effect on the efferent phase of the autoimmune response, in particular in the CNS.

We propose that MIF blockade impaired the homing and transmigration of neuroantigen-reactive T cells to the CNS. As a consequence, the autoreactive T cells were deprived of TCR and costimulatory molecule-mediated signals necessary for cell activation and/or survival (47–49). Deprived of these signals, the $PLP_{139-151}$-reactive T cells may have become more susceptible to apoptotic cell death or induction of anergy. Interestingly, VLA-4, the ligand for VCAM-1, has been reported to function as a costimulatory molecule (50, 51) and to protect T cells from apoptosis (45). Importantly, the increase in the activation threshold of $PLP_{139-151}$-specific T cells was also observed when T cells from anti-MIF Ab-injected mice were stimulated with spleen cells from naive mice (not Ab treated, Figs. 5*b* and 6*b*) as APCs. Hence, the alterations of T cell effector functions induced by the MIF blockade could not be overcome by normal APCs. However, the anti-MIF Ab treatment could have affected APC effector functions in addition, which we have not yet tested.

Recently, regulatory cells have received renewed interest in the control of autoimmunity (52). Therefore, we tested whether or not a deviation toward the production of regulatory Th2 cytokines occurred in this model, as has been reported for experimental models using mAbs to block B7-1 (53). As shown in Fig. 5, we did not observe a switch toward the production of IL-4, IL-5, or IL-10. Moreover, we found that T cells from anti-MIF Ab-treated mice were not protective (C. Denkinger and T. Forsthuber, unpublished observations), although we did not directly test for TGF-β produced by Th3 cells, or $CD25^+$ regulatory T cells (54). Thus, we hypothesize that the efficacy of anti-MIF Abs in the treatment of EAE is primarily due to its down-modulatory effect on the autoimmune Th1 response.

Importantly, our results showed that anti-MIF Ab treatment was efficacious after the onset of clinical EAE symptoms, and that the effects were not mouse strain- or neuroantigen-dependent. Thus, anti-MIF Abs could provide a promising novel therapy for the treatment of acute MS without requiring exact knowledge of the nature of the neuroantigens targeted by the autoimmune T cells. This is a major advantage over other current attempts at Ag-specific immunotherapies, such as altered peptide ligands.

Acknowledgments

We thank Drs. A. Stavitsky, Edward Spack, and K. Weichsel for critically reading the manuscript, Dr. E. Pearlman for help with the VCAM-1 staining, and Carey Shive and Rocio Guardia for excellent technical assistance. This work is part of the doctoral thesis of C. Denkinger and is supported by Dr. Thomas Huenig (Institute of Virology and Immunology, University of Würzburg).

References

1. Rivers, T. M., and F. F. Schwentker. 1935. Encephalomyelitis accompanied by myelin destruction experimentally produced in monkeys. *J. Exp. Med. 61:689.*
2. Steinman, L. 1996. Multiple sclerosis: a coordinated immunological attack against myelin in the central nervous system. *Cell 85:299.*
3. Mendel, I., d. R. Kerlero, and A. Ben Nun. 1995. A myelin oligodendrocyte glycoprotein peptide induces typical chronic experimental autoimmune encephalomyelitis in H-2^b mice: fine specificity and T cell receptor Vβ expression of encephalitogenic T cells. *Eur. J. Immunol. 25:1951.*
4. Yednock, T. A., C. Cannon, L. C. Fritz, F. Sanchez-Madrid, L. Steinman, and N. Karin. 1992. Prevention of experimental autoimmune encephalomyelitis by antibodies against $\alpha_4\beta_1$ integrin. *Nature 356:63.*
5. Karpus, W. J., N. W. Lukacs, B. L. McRae, R. M. Strieter, S. L. Kunkel, and S. D. Miller. 1995. An important role for the chemokine macrophage inflammatory protein-1α in the pathogenesis of the T cell-mediated autoimmune disease, experimental autoimmune encephalomyelitis. *J. Immunol. 155:5003.*
6. Glabinski, A. R., S. O'Bryant, K. Selmaj, and R. M. Ransohoff. 2000. CXC chemokine receptors expression during chronic relapsing experimental autoimmune encephalomyelitis. *Ann. NY Acad. Sci. 917:135.*
7. David, J. R. 1966. Delayed hypersensitivity in vitro: its mediation by cell-free substances formed by lymphoid cell-antigen interaction. *Proc. Natl. Acad. Sci. USA 56:72.*
8. Bloom, B. R., and B. Bennett. 1966. Mechanism of a reaction in vitro associated with delayed-type hypersensitivity. *Science 153:80.*
9. Calandra, T., J. Bernhagen, R. A. Mitchell, and R. Bucala. 1994. The macrophage is an important and previously unrecognized source of macrophage migration inhibitory factor. *J. Exp. Med. 179:1895.*
10. Nishino, T., J. Bernhagen, H. Shiiki, T. Calandra, K. Dohi, and R. Bucala. 1995. Localization of macrophage migration inhibitory factor (MIF) to secretory granules within the corticotrophic and thyrotrophic cells of the pituitary gland. *Mol. Med. 1:781.*
11. Weiser, W. Y., P. A. Temple, J. S. Witek-Giannotti, H. G. Remold, S. C. Clark, and J. R. David. 1989. Molecular cloning of a cDNA encoding a human macrophage migration inhibitory factor. *Proc. Natl. Acad. Sci. USA 86:7522.*
12. Bernhagen, J., R. A. Mitchell, T. Calandra, W. Voelter, A. Cerami, and R. Bucala. 1994. Purification, bioactivity, and secondary structure analysis of mouse and human macrophage migration inhibitory factor (MIF). *Biochemistry 33:14144.*
13. Bacher, M., C. N. Metz, T. Calandra, K. Mayer, J. Chesney, M. Lohoff, D. Gemsa, T. Donnelly, and R. Bucala. 1996. An essential regulatory role for macrophage migration inhibitory factor in T-cell activation. *Proc. Natl. Acad. Sci. USA 93:7849.*
14. Mikulowska, A., C. N. Metz, R. Bucala, and R. Holmdahl. 1997. Macrophage migration inhibitory factor is involved in the pathogenesis of collagen type II-induced arthritis in mice. *J. Immunol. 158:5514.*
15. Lan, H. Y., N. Yang, C. Metz, W. Mu, Q. Song, D. J. Nikolic-Paterson, M. Bacher, R. Bucala, and R. C. Atkins. 1997. TNF-α up-regulates renal MIF expression in rat crescentic glomerulonephritis. *Mol. Med. 3:136.*
16. Mizue, Y., J. Nishihira, T. Miyazaki, S. Fujiwara, M. Chida, K. Nakamura, K. Kikuchi, and M. Mukai. 2000. Quantitation of macrophage migration inhibitory factor (MIF) using the one-step sandwich enzyme immunosorbent assay: elevated serum MIF concentrations in patients with autoimmune diseases and identification of MIF in erythrocytes. *Int. J. Mol. Med. 5:397.*
17. Niino, M., A. Ogata, S. Kikuchi, K. Tashiro, and J. Nishihira. 2000. Macrophage migration inhibitory factor in the cerebrospinal fluid of patients with conventional and optic-spinal forms of multiple sclerosis and neuro-Behcet's disease. *J. Neurol. Sci. 179:127.*
18. Bacher, M., A. Meinhardt, H. Y. Lan, F. S. Dhabhar, W. Mu, C. N. Metz, J. A. Chesney, D. Gemsa, T. Donnelly, R. C. Atkins, and R. Bucala. 1998. MIF expression in the rat brain: implications for neuronal function. *Mol. Med. 4:217.*
19. Galat, A., S. Riviere, F. Bouet, and A. Menez. 1994. A diversified family of 12-kDa proteins with a high amino acid sequence similarity to macrophage migration-inhibitory factor (MIF). *Eur. J. Biochem. 224:417.*
20. Chesney, J., C. Metz, M. Bacher, T. Peng, A. Meinhardt, and R. Bucala. 1999. An essential role for macrophage migration inhibitory factor (MIF) in angiogenesis and the growth of a murine lymphoma. *Mol. Med. 5:181.*
21. Rocken, M., M. Racke, and E. M. Shevach. 1996. IL-4 induced immune deviation as antigen-specific therapy for inflammatory autoimmune disease. *Immunol. Today 17:225.*
22. Lehmann, P. V., T. Forsthuber, A. Miller, and E. E. Sercarz. 1992. Spreading of T-cell autoimmunity to cryptic determinants of an autoantigen. *Nature 358:155.*
23. Shive, C. L., H. Hofstetter, L. Arredondo, C. Shaw, and T. G. Forsthuber. 2000. The enhanced antigen-specific production of cytokines induced by pertussis toxin is due to clonal expansion of T cells and not to altered effector functions of long-term memory cells. *Eur. J. Immunol. 30:2422.*
24. Karulin, A. Y., M. D. Hesse, M. Tary-Lehmann, and P. V. Lehmann. 2000. Single-cytokine-producing CD4 memory cells predominate in type 1 and type 2 immunity. *J. Immunol. 164:1862.*
25. Yip, H. C., A. Y. Karulin, M. Tary-Lehmann, M. D. Hesse, H. Radeke, P. S. Heeger, R. P. Trezza, F. P. Heinzel, T. Forsthuber, and P. V. Lehmann. 1999. Adjuvant-guided type-1 and type-2 immunity: infectious/noninfectious dichotomy defines the class of response. *J. Immunol. 162:3942.*
26. Racke, M. K., S. Dhib-Jalbut, B. Cannella, P. S. Albert, C. S. Raine, and D. E. McFarlin. 1991. Prevention and treatment of chronic relapsing experimental allergic encephalomyelitis by transforming growth factor-β1. *J. Immunol. 146:3012.*
27. Kort, J. J. 1998. Impairment of excitatory amino acid transport in astroglial cells infected with the human immunodeficiency virus type 1. *AIDS Res. Hum. Retroviruses 14:1329.*
28. Kaifi, J. T., E. Diaconu, and E. Pearlman. 2001. Distinct roles for PECAM-1, ICAM-1, and VCAM-1 in recruitment of neutrophils and eosinophils to the cornea in ocular onchocerciasis (river blindness). *J. Immunol. 166:6795.*
29. Greenwood, J., Y. Wang, and V. L. Calder. 1995. Lymphocyte adhesion and transendothelial migration in the central nervous system: the role of LFA-1, ICAM-1, VLA-4 and VCAM-1: off. *Immunology 86:408.*
30. Steffen, B. J., E. C. Butcher, and B. Engelhardt. 1994. Evidence for involvement of ICAM-1 and VCAM-1 in lymphocyte interaction with endothelium in experimental autoimmune encephalomyelitis in the central nervous system in the SJL/J mouse. *Am. J. Pathol. 145:189.*
31. Brocke, S., C. Piercy, L. Steinman, I. L. Weissman, and T. Veromaa. 1999. Antibodies to CD44 and integrin α_4, but not L-selectin, prevent central nervous system inflammation and experimental encephalomyelitis by blocking secondary leukocyte recruitment. *Proc. Natl. Acad. Sci. USA 96:6896.*
32. Hori, J., M. Isobe, S. Yamagami, and T. Tsuru. 1998. Acceptance of second corneal allograft by combination of anti-VLA-4 and anti-LFA-1 monoclonal antibodies in mice. *Transplant. Proc. 30:200.*
33. Irani, D. N., and D. E. Griffin. 1996. Regulation of lymphocyte homing into the brain during viral encephalitis at various stages of infection. *J. Immunol. 156: 3850.*
34. Qing, Z., M. Sandor, Z. Radvany, D. Sewell, A. Falus, D. Potthoff, W. A. Muller, and Z. Fabry. 2001. Inhibition of antigen-specific T cell trafficking into the central nervous system via blocking PECAM1/CD31 molecule. *J. Neuropathol. Exp. Neurol. 60:798.*
35. Carrithers, M. D., I. Visintin, S. J. Kang, and C. A. Janeway, Jr. 2000. Differential adhesion molecule requirements for immune surveillance and inflammatory recruitment. *Brain 123:1092.*
36. Lan, H. Y., M. Bacher, N. Yang, W. Mu, D. J. Nikolic-Paterson, C. Metz, A. Meinhardt, R. Bucala, and R. C. Atkins. 1997. The pathogenic role of macrophage migration inhibitory factor in immunologically induced kidney disease in the rat. *J. Exp. Med. 185:1455.*
37. Theien, B. E., C. L. Vanderlugt, T. N. Eagar, C. Nickerson-Nutter, R. Nazareno, V. K. Kuchroo, and S. D. Miller. 2001. Discordant effects of anti-VLA-4 treatment before and after onset of relapsing experimental autoimmune encephalomyelitis. *J. Clin. Invest. 107:995.*
38. Wildbaum, G., N. Netzer, and N. Karin. 2002. Plasmid DNA encoding IFN-γ-inducible protein 10 redirects antigen-specific T cell polarization and suppresses experimental autoimmune encephalomyelitis. *J. Immunol. 168:5885.*
39. Fife, B. T., K. J. Kennedy, M. C. Paniagua, N. W. Lukacs, S. L. Kunkel, A. D. Luster, and W. J. Karpus. 2001. CXCL10 (IFN-γ-inducible protein-10) control of encephalitogenic $CD4^+$ T cell accumulation in the central nervous system during experimental autoimmune encephalomyelitis. *J. Immunol. 166: 7617.*
40. Karpus, W. J., and K. J. Kennedy. 1997. MIP-1α and MCP-1 differentially regulate acute and relapsing autoimmune encephalomyelitis as well as Th1/Th2 lymphocyte differentiation. *J. Leukocyte Biol. 62:681.*
41. Kennedy, K. J., R. M. Strieter, S. L. Kunkel, N. W. Lukacs, and W. J. Karpus. 1998. Acute and relapsing experimental autoimmune encephalomyelitis are regulated by differential expression of the CC chemokines macrophage inflammatory protein-1α and monocyte chemotactic protein-1. *J. Neuroimmunol. 92:98.*
42. Dufour, J. H., M. Dziejman, M. T. Liu, J. H. Leung, T. E. Lane, and A. D. Luster. 2002. IFN-γ-inducible protein 10 (IP-10; CXCL10)-deficient mice reveal a role for IP-10 in effector T cell generation and trafficking. *J. Immunol. 168:3195.*
43. Murakami, H., S. M. Akbar, H. Matsui, N. Horiike, and M. Onji. 2002. Macrophage migration inhibitory factor activates antigen-presenting dendritic cells and induces inflammatory cytokines in ulcerative colitis. *Clin. Exp. Immunol. 128:504.*

44. Hermanowski-Vosatka, A., S. S. Mundt, J. M. Ayala, S. Goyal, W. A. Hanlon, R. M. Czerwinski, S. D. Wright, and C. P. Whitman. 1999. Enzymatically inactive macrophage migration inhibitory factor inhibits monocyte chemotaxis and random migration. *Biochemistry 38:12841.*
45. Zaitseva, M. B., C. F. Mojcik, D. R. Salomon, E. M. Shevach, and H. Golding. 1998. Co-ligation of $\alpha_4\beta_1$ integrin and TCR rescues human thymocytes from steroid-induced apoptosis. *Int. Immunol. 10:1551.*
46. Targoni, O. S., and P. V. Lehmann. 1998. Endogenous myelin basic protein inactivates the high avidity T cell repertoire. *J. Exp. Med. 187:2055.*
47. Radvanyi, L. G., Y. Shi, H. Vaziri, A. Sharma, R. Dhala, G. B. Mills, and R. G. Miller. 1996. CD28 costimulation inhibits TCR-induced apoptosis during a primary T cell response. *J. Immunol. 156:1788.*
48. Collette, Y., D. Razanajaona, M. Ghiotto, and D. Olive. 1997. CD28 can promote T cell survival through a phosphatidylinositol 3-kinase-independent mechanism. *Eur. J. Immunol. 27:3283.*
49. Walker, L. S., J. D. McLeod, G. Boulougouris, Y. I. Patel, N. D. Hall, and D. M. Sansom. 1998. Down-regulation of CD28 via Fas (CD95): influence of CD28 on T-cell apoptosis. *Immunology 94:41.*
50. Damle, N. K., and A. Aruffo. 1991. Vascular cell adhesion molecule 1 induces T-cell antigen receptor-dependent activation of $CD4^+$ T lymphocytes. *Proc. Natl. Acad. Sci. USA 88:6403.*
51. Damle, N. K., K. Klussman, G. Leytze, H. D. Ochs, A. Aruffo, P. S. Linsley, and J. A. Ledbetter. 1993. Costimulation via vascular cell adhesion molecule-1 induces in T cells increased responsiveness to the CD28 counter-receptor B7. *Cell. Immunol. 148:144.*
52. Maloy, K. J., and F. Powrie. 2001. Regulatory T cells in the control of immune pathology. *Nat. Immunol. 2:816.*
53. Kuchroo, V. K., M. P. Das, J. A. Brown, A. M. Ranger, S. S. Zamvil, R. A. Sobel, H. L. Weiner, N. Nabavi, and L. H. Glimcher. 1995. B7-1 and B7-2 costimulatory molecules activate differentially the Th1/Th2 developmental pathways: application to autoimmune disease therapy. *Cell 80:707.*
54. Miller, A., O. Lider, A. B. Roberts, M. B. Sporn, and H. L. Weiner. 1992. Suppressor T cells generated by oral tolerization to myelin basic protein suppress both in vitro and in vivo immune responses by the release of transforming growth factor-β after antigen-specific triggering. *Proc. Natl. Acad. Sci. USA 89:421.*